

EVALUATION OF THE ROLE OF REACTIVE OXYGEN SPECIES IN PMC-BASED OXIDATION SYSTEMS FOR RB21 DYE DEGRADATION

Vu Thi Tinh and Nguyen Thi Bich Viet*

Faculty of Chemistry, Hanoi National University of Education, Hanoi city, Vietnam

*Corresponding author: Nguyen Thi Bich Viet, e-mail: vietntb@hnue.edu.vn

Received October 5, 2024. Revised October 24, 2024. Accepted October 31, 2024.

Abstract. This work aimed to evaluate the contribution of reactive oxygen species (ROS) in a green oxidation system based on peroxymonocarbonate (PMC) to the degradation efficiency of RB21 textile dye using ROS scavengers such as t-butanol, terephthalic acid (TA), *N,N*-dimethylaniline (DMA), ascorbic acid. The results showed that in reaction conditions including RB21 dye 4.63×10^{-2} mM (50 mg/L); HCO_3^- 50 mM; H_2O_2 100 mM; Co^{2+} 1.70×10^{-3} mM (0.1 mg/L), the RB21 degradation efficiency reached 90% after 180 minutes of which the contribution percentage of $\text{CO}_3^{\cdot-}$ radicals was the most important, 98.2%, while $\cdot\text{OH}$ and other ROS hardly contributed to the degradation process of RB21 dye. Moreover, the kinetic study results on the reaction between $\text{CO}_3^{\cdot-}$ and its scavenger, DMA, as well as between $\cdot\text{OH}$ and its scavenger, TA, indicated that the concentrations of $\text{CO}_3^{\cdot-}$ and $\cdot\text{OH}$ in the PMC system composed of HCO_3^- 50 mM, H_2O_2 100 mM, and Co^{2+} 1.70×10^{-3} mM were $2.35 \cdot 10^{-13}$ M and $1.50 \cdot 10^{-16}$ M, respectively.

Keywords: RB21 dye, PMC, reactive oxygen species, scavengers.

1. Introduction

In recent years, advanced oxidation processes (AOPs) based on peroxymonocarbonate (PMC) have been proven to be remarkably effective in treating harmful organic substances such as phenol [1], methyl orange (MO), rhodamine B (RhB) [2], acid orange 7 (AO7) [3], or acid orange 8 (AO8) [4], methylene blue (MB) [5], reactive blue (RB21) [6], reactive blue 19 (RB19) [7] with short treating times and completely mineralized products. Compared to other advanced oxidation systems like Fenton ($\text{Fe}^{2+}/\text{H}_2\text{O}_2$), $\text{H}_2\text{O}_2/\text{O}_3$, $\text{H}_2\text{O}_2/\text{UV}$, and O_3/UV , the PMC systems, typically formed *in situ* by the cobalt(II)-catalyzed reaction between bicarbonate and hydrogen peroxide, produce more reactive oxygen species (ROS) including PMC (HCO_4^-), carbonate anion radical ($\text{CO}_3^{\cdot-}$), singlet oxygen ($^1\text{O}_2$), superoxide ($\text{O}_2^{\cdot-}$), hydroxyl ($\cdot\text{OH}$), and hydroperoxyl ($\cdot\text{HO}_2$) radicals. Unfortunately, these ROS are responsible for the degradation of pollutants in AOPs. Therefore, it is vital to understand the formation of ROS in the PMC systems and

their contributions to pollutant degradation efficiency. For this purpose, one of the possible approaches is using quenching agents, so-called radical scavengers [8], such as *t*-butanol ($\cdot\text{OH}$ scavengers) [9], terephthalic acid ($\cdot\text{OH}$ scavenger) [10], *N,N*-dimethylaniline ($\text{CO}_3^{\cdot-}$ scavenger) [11], ascorbic acid (scavenger of most radicals) [12]. Among them, terephthalic acid (TA), a non-fluorescent compound, was reported to react selectively with $\cdot\text{OH}$ with a rate constant of $4.4 \times 10^9 \text{ M}^{-1} \text{ s}^{-1}$ to produce hydroxylterephthalic acid (hTA), a fluorescent product, suitable for a photometric determination [10]. Whereas, *N,N*-dimethylaniline (DMA), a fluorescent substance, was reported to be a selective probe for $\text{CO}_3^{\cdot-}$ radical that generates a non-fluorescent product [11].

The literature review has indicated that the dominant reactive oxygen species produced in the PMC systems depended on the composition of the systems and the pollutants being treated. It was reported that $\text{CO}_3^{\cdot-}$ radicals played a key role in the degradation of AO8 (T. Zhao *et al.*) [4], whereas $\cdot\text{OH}$ radicals played a decisive role in treating MB (A. Xu *et al.*) [5]. However, another study on MB degradation by A. Xu *et al.* showed that in a transition-metal-free PMC system (without Co^{2+}), $\text{O}_2^{\cdot-}$ might play this key role [2]. Although these findings are interesting, information on the concentration of these reactive species in the PMC systems is essential to clarify the organic compound degradation mechanism of the PMC systems, however to date, no literature has been found on ROS quantification in advanced oxidation systems like PMC.

In our previous study on RB21 textile dye degradation by PMC systems, it was interesting to notice that the dye treatment efficiency could reach $> 90\%$ within 180 minutes and even much shorter (30 minutes) when using UV irradiation [6]. Yet neither the role of ROS in the RB21 degradation nor their quantification has been investigated.

To address the above unresolved issues, the present work focuses on (i) determining the contribution percentage of each reactive species to the degradation efficiency of RB21, and (ii) quantifying two major reactive species in the PMC system, $\text{CO}_3^{\cdot-}$ and $\cdot\text{OH}$ radicals.

2. Content

2.1. Experiments

2.1.1. Chemicals and instruments

All chemicals used in this work such as sodium bicarbonate, hydrogen peroxide, cobalt nitrate, *t*-butanol, *N,N*-dimethylaniline, terephthalic acid, ascorbic acid, and reactive blue 21 were of analytical grade and purchased from Sigma Aldrich.

A Genesys 30 Visible spectrophotometer (Thermo Scientific) and an FL8500 Fluorescence spectrophotometer (Perkin Elmer) were used to monitor the absorbance and the fluorescence emission of the reaction solutions, respectively.

2.1.2. Investigation of RB21 degradation by PMC oxidation system in the absence and presence of ROS quenchers

All RB21 degradation experiments were carried out in a 250-mL reactor under magnetic stirring at $25 \pm 1 \text{ }^\circ\text{C}$ with common reaction conditions including NaHCO_3 50 mM; H_2O_2 100 mM; Co^{2+} 1.7×10^{-3} mM; pH ~ 9 (inherently buffered); RB21 dye 4.63×10^{-2} mM (50 mg/L). The addition of corresponding scavengers (Entries 2 \div 9) was conducted before adding RB21 dye. Other experiment conditions were specified in Table 1.

To monitor the variation of RB21 concentration over time, after a time t , about 3 mL of the reaction mixture was withdrawn to measure the absorbance at 625 nm. The dye concentration at different reaction times was obtained from the 625-nm absorbance of the dye solution according to the following equation: $A_{625\text{nm}} = (1.83 \pm 0.07) \cdot 10^{-5} \cdot C_{\text{RB21}}$ (mM) with $R^2 = 0.9999$, LOD = 9.91×10^{-4} mM, LOQ = 2.97×10^{-3} mM with a linear range from 1.85×10^{-3} mM to 0.0926 mM. The RB21 degradation efficiency (H%) was calculated using the formula $H\% = \frac{C_0 - C_t}{C_0} \times 100$ where C_0 and C_t are the initial concentration and the concentration at time t of RB21, respectively.

Table 1. Experiment conditions to investigate the contribution percentage of each ROS to the RB21 degradation efficiency

Entry #	Experiment	ROS scavenger (C _M)
1	Comparison system	Absence of scavenger
2 ÷ 3	Presence of $\cdot\text{OH}$ scavenger	<i>t</i> -butanol (0.01; 0.50 M)
4 ÷ 6	Presence of $\text{CO}_3^{\cdot-}$ scavenger	DMA (0.0825; 0.4126; 1.6503 mM)
7 ÷ 9	Presence of most ROS scavenger	Ascorbic acid (1; 5; 10 mM)

2.1.3. Kinetic study of ROS quenching experiments

All experiments were carried out in a 100-mL reactor under magnetic stirring at 25 ± 1 °C. The composition of the PMC system consists of HCO_3^- 50 mM; H_2O_2 100 mM; Co^{2+} 1.70×10^{-3} mM. Based on preliminary studies, TA was used as $\cdot\text{OH}$ scavenger and its concentration was fixed at 9.90×10^{-2} mM. DMA was used as $\text{CO}_3^{\cdot-}$ scavenger and its concentration was fixed at 0.66 mM. After a time t , about 0.5 mL of the reaction mixture was taken out to measure the fluorescence emission. The conditions of quenching experiments are shown in Table 2.

Table 2. Quenching experiments conditions for kinetic study

Entry #	Experiment	Scavenger	Fluorophore	Measurement condition
1	Determination of $\cdot\text{OH}$ radicals	TA 9.90×10^{-2} mM	hTA	$\lambda_{\text{ex}} = 315$ nm, $\lambda_{\text{em}} = 425$ nm, slit width 5 nm, source energy 550V
2	Determination of $\text{CO}_3^{\cdot-}$ radicals	DMA 0.66 mM	DMA	$\lambda_{\text{ex}} = 298$ nm, $\lambda_{\text{em}} = 360$ nm, slit width 5 nm, source energy 400V

2.2. Results and discussion

2.2.1. Evaluating the contribution of ROS in the PMC system to RB21 degradation

To determine the contribution percentage of each reactive species, RB21 degradation efficiency was investigated in the absence and presence of corresponding scavengers. The experimental procedure was modified based on the literature [7]. The general principle to evaluate the contribution of a reactive species present in the PMC system to RB21 degradation is to compare the dye degradation efficiencies in the absence of scavengers (The comparison system) and in the presence of the scavenger of corresponding ROS.

For this purpose, a first-order kinetic model was applied to the degradation reaction of RB21 dye to determine the contribution of ROS in the PMC system such as $\cdot\text{OH}$, $\text{CO}_3^{\cdot-}$, and other reactive species. The application of the kinetic model in each quenching experiment is described as follows:

- In the absence of scavengers:

$$-\frac{d[\text{RB21}]}{dt} = k_0 \times [\text{RB21}]$$

- In the presence of *t*-butanol ($\cdot\text{OH}$ scavenger):

$$-\frac{d[\text{RB21}]}{dt} = k_{01} \times [\text{RB21}]$$

- In the presence of DMA ($\text{CO}_3^{\cdot-}$ scavenger):

$$-\frac{d[\text{RB21}]}{dt} = k_{02} \times [\text{RB21}]$$

- In the presence of ascorbic acid (scavenger of most ROS):

$$-\frac{d[\text{RB21}]}{dt} = k_{03} \times [\text{RB21}]$$

where k_0 , k_{01} , k_{02} , and k_{03} are the observed first-order rate constants of the RB21 degradation reaction in the absence and presence of *t*-butanol, DMA, and ascorbic acid, respectively.

The contribution percentage of reactive species can be calculated using the corresponding formula in Table 3.

Table 3. Formula to calculate the contribution percentage of ROS in the PMC system to RB21 degradation efficiency

% contribution of	$\cdot\text{OH}$	$\text{CO}_3^{\cdot-}$	most ROS
Formula	$\frac{k_0 - k_{01}}{k_0}$	$\frac{k_0 - k_{02}}{k_0}$	$\frac{k_0 - k_{03}}{k_0}$

*** Contribution of $\cdot\text{OH}$ in the PMC system to RB21 degradation efficiency**

The results of $\cdot\text{OH}$ quenching experiments using *t*-butanol as the $\cdot\text{OH}$ scavenger are presented in Figure 1.

Figure 1(a) indicates that the presence of *t*-butanol at low or high concentrations (0.01 or 0.50 M) hardly affected the RB21 degradation efficacy of the PMC system. In all cases, the RB21 degradation efficiency reached about 90% after 180 minutes. The plots in Figure 1(b) allow determining the contribution percentage of $\cdot\text{OH}$ as 0% because both the rate constant of the RB21 degradation reaction in the absence and in the presence of *t*-butanol was equal to 0.017 s^{-1} ($k_0 = k_{01}$). It can be concluded that in the degradation process of RB21 by the PMC system, the role of $\cdot\text{OH}$ radical was negligible. This result is consistent with the study of AO7 degradation by Y. Li *et al.* [3] and AO8 degradation by T. Zhao *et al.* [4].

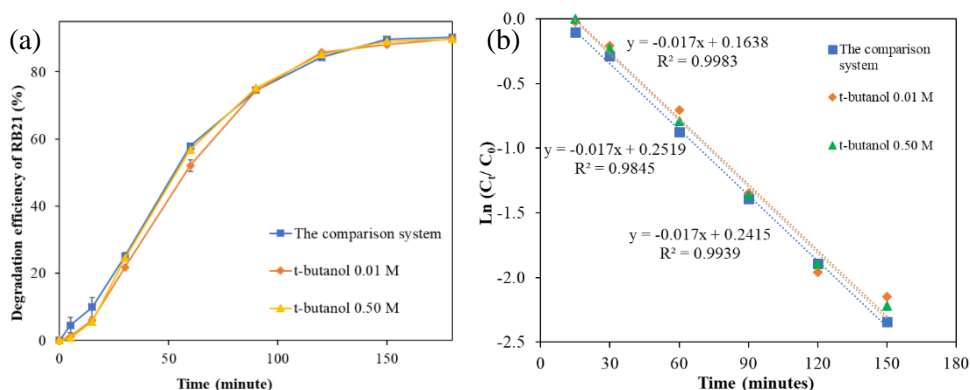


Figure 1. Kinetic investigation of RB21 degradation at different concentrations of t-butanol: (a) RB21 degradation efficiency and (b) $\ln(C_t/C_0)$ over time

*** Contribution of $CO_3^{\cdot-}$ in the PMC system to RB21 degradation efficiency**

The results of $CO_3^{\cdot-}$ quenching experiments using DMA as the $CO_3^{\cdot-}$ scavenger are presented in Figure 2.

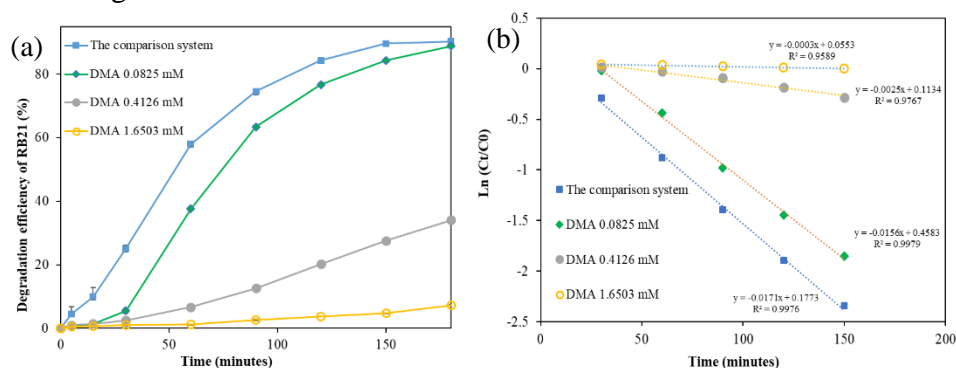


Figure 2. Kinetic investigation of RB21 degradation at different concentrations of DMA: (a) RB21 degradation efficiency and (b) $\ln(C_t/C_0)$ over time

Figure 2(a) shows that an increase in DMA concentration from 0.0825 to 1.6503 M resulted in a dramatic diminution of RB21 degradation efficiency. Compared to the comparison system (without scavenger), after 180 minutes of reaction, the RB21 degradation efficiency decreased from 90% to 7.3%. Figure 2 (b) reveals that the rate constant of the RB21 degradation reaction at 1.6503 M of DMA was 0.0003 s^{-1} (k_2) while the one of the comparison system was 0.017 s^{-1} (k_0), therefore the contribution percentage of $CO_3^{\cdot-}$ radicals calculated was 98.2% according to the formula in Table 3. This result revealed that the $CO_3^{\cdot-}$ radicals played a key role in the degradation of RB21 by the PMC system. This finding is consistent with the study of T. Zhao *et al.* [4].

*** Contribution of other reactive species in the PMC system to RB21 degradation efficiency**

It can be deduced from the results obtained that the contribution of other reactive species in the PMC system to the degradation of RB21 was insignificant, less than 2%. This finding was confirmed by the results obtained with the quenching experiment using

ascorbic acid as the scavenger of most ROS, as shown in Figure 3. As seen in Figures 3(a) and 3(b), at an ascorbic acid concentration of 10 mM, most of the reactive species in the PMC system were quenched and the degradation efficiency of RB21 was 0%.

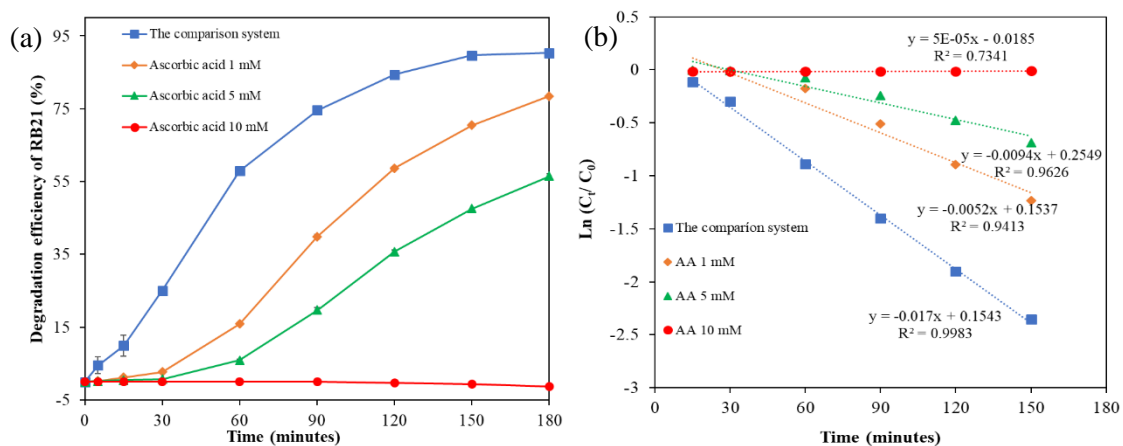


Figure 3. Kinetic investigation of RB21 degradation at different concentrations of AA: (a) RB21 degradation efficiency and (b) $\ln(C_t/C_0)$ over time

2.2.2. Quantification of $\cdot\text{OH}$ and $\text{CO}_3^{\cdot-}$ radicals in the PMC system

* Quantification of $\cdot\text{OH}$ radicals

The reaction between $\cdot\text{OH}$ radicals and TA has been reported to be a second-order reaction with rate constant $k_1 = 4.4 \times 10^9 \text{ M}^{-1} \text{ s}^{-1}$ [10]. The reaction produces hydroxyterephthalic acid (hTA) that emits maximum fluorescence intensity at 425 nm (λ_{em}) when excited at 315 nm (λ_{ex}). The kinetic equation of the reaction between $\cdot\text{OH}$ and TA can be described as follows:

$$-\ln \frac{C_{TA}^t}{C_{TA}^0} = k_1 \times C_{OH\cdot} \times t = k_1' \times t$$

where C_{TA}^0 and C_{TA}^t are the initial concentration and the concentration at time t of TA; $C_{OH\cdot}$ is the steady-state concentration of $\cdot\text{OH}$ radicals; k_1' is the observed rate constant of the reaction between $\cdot\text{OH}$ with TA, $k_1' = k_1 \times C_{OH\cdot} = 4.4 \times 10^9 \times C_{OH\cdot}$.

C_{TA}^0 and C_{TA}^t are related to each other by the equation: $C_{TA}^t = C_{TA}^0 - C_{hTA}^t$, where C_{hTA}^t is the concentration of hTA at time t , which can be determined by measuring fluorescence intensity ($I_{425\text{nm}}$) using a calibration curve: $I_{425\text{nm}} = (965 \pm 0.957) \times C_{hTA} (\text{mM}) + (83 \pm 19)$ with $R^2 = 0.99998$, LOD = 5.36×10^{-6} mM, LOQ = 1.61×10^{-5} mM, in a dynamic range from 6.02×10^{-5} mM to 1.20×10^{-3} mM.

By plotting $\ln \frac{C_{TA}^t}{C_{TA}^0}$ versus time t , the observed rate constant k_1' can be determined, and thus the steady-state concentration of $\cdot\text{OH}$ radicals can be deduced.

Fluorescence analysis results in Figure 4(a) show that the fluorescence intensity of hTA at 425 nm increased from 777 AU to 9873 AU when the reaction time increased from 4 to 90 minutes. This proves that hTA was formed in the reaction system with increasing concentration over time. The plot of $\ln(C_t/C_0)$ vs. t in Figure 4(b) indicates the best fit to the first-order kinetic model for TA concentration with $k_1' = 4.035 \times 10^{-5} \text{ min}^{-1}$ ($= 6.725 \times 10^{-6} \text{ s}^{-1}$) with $R^2 = 0.9994$. As a result, the steady-state concentration of $\cdot\text{OH}$ radical was determined to be $1.50 \times 10^{-16} \text{ M}$, which aligns with the negligible contribution of this radical to the RB21 degradation by the PMC oxidation system as discussed in 2.2.1.

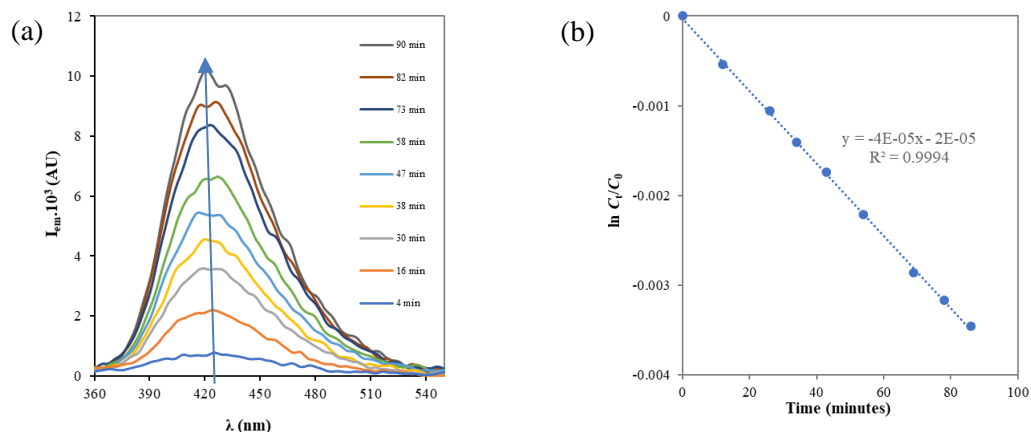


Figure 4. Determination of $\cdot\text{OH}$ radicals using TA as $\cdot\text{OH}$ scavenger:
(a) Fluorescence spectra of hTA at different reaction times; (b) $\ln(C_t/C_0)$ vs. t

* Quantification of $\text{CO}_3^{\cdot-}$ radicals

It was reported that DMA can react selectively with $\text{CO}_3^{\cdot-}$ radicals with a rate constant $k_2 = 1.8 \times 10^9 \text{ M}^{-1}\text{s}^{-1}$ [13]. DMA is a fluorescence probe that emits maximum fluorescence intensity at $\lambda_{\text{em}} = 360 \text{ nm}$ when excited at $\lambda_{\text{ex}} = 298 \text{ nm}$. Different from the above method of determining $\cdot\text{OH}$, $\text{CO}_3^{\cdot-}$ radicals were analyzed by measuring the remaining DMA concentration in the reaction solution at time t via the equation: $-\ln \frac{I_t}{I_0} = k_2' \times t$, where I_0 and I_t are the fluorescence intensities at 360 nm measured at the initial time and time t ; $k_2' = 1.8 \times 10^9 \times C_{\text{CO}_3^{\cdot-}}$ ($C_{\text{CO}_3^{\cdot-}}$ is the steady-state concentration of $\text{CO}_3^{\cdot-}$).

The results obtained in the experiment using DMA as $\text{CO}_3^{\cdot-}$ scavenger are presented in Figure 5. Fluorescence spectra recorded at different reaction times in Figure 5(a) all show a fluorescence emission peak at a wavelength of about 360 nm, corresponding to the emission wavelength of DMA. The peak intensity decreased by 75.3% from 102137 AU to 25201 AU when the reaction time increased to 56 minutes, meaning that a large amount of $\text{CO}_3^{\cdot-}$ radicals were produced in the mixture during this time. The plot of $\ln(I_t/I_0)$ vs. t in Figure 5(b) demonstrates good linearity for the first-order kinetic model for DMA concentration with $k_2' = 0.0253 \text{ min}^{-1}$ ($= 4.217 \times 10^{-4} \text{ s}^{-1}$) with $R^2 = 0.9899$.

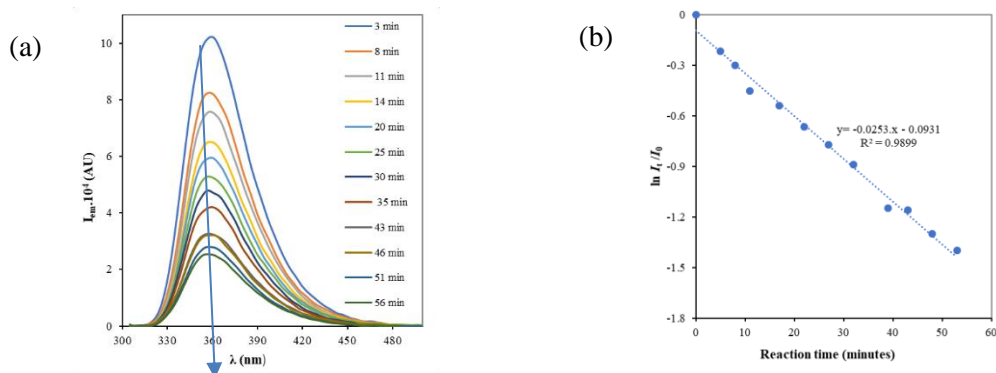


Figure 5. Determination of $\text{CO}_3^{\bullet-}$ radicals using DMA as $\text{CO}_3^{\bullet-}$ scavenger: (a) Fluorescence spectra of DMA at different reaction times; (b) $\ln(I_t/I_0)$ vs. t

Therefore, the steady-state concentration was determined to be 2.35×10^{-13} M, 1000 times higher than the steady-state concentration of $\cdot\text{OH}$. This finding is consistent with the results discussed in 2.2.1 about the major contribution of carbonate radicals in the RB21 degradation by the PMC system.

To sum up, in the PMC system, the carbonate radical anion is mainly responsible for the efficacy of the RB21 degradation process. This can be explained not only by its 1000-fold higher concentration compared to hydroxyl radical but also by its higher selectivity toward organic pollutants containing electron-rich groups like RB21 dye. Whereas, hydroxyl radical is well-known as a non-selective strong oxidant. Another reason for that may be the much longer lifetime of carbonate radical anion compared to hydroxyl radicals in the AOPs [13].

3. Conclusions

In this study, the contribution of reactive species in the PMC system to RB21 degradation efficiency was investigated. The results showed that, $\text{CO}_3^{\bullet-}$ radicals play a decisive role in the degradation of RB21 with a dominant contribution of 98.2%, while $\cdot\text{OH}$ radicals and other reactive species only contributed insignificantly in the RB21 degradation process. The steady-state concentration of $\text{CO}_3^{\bullet-}$ radicals were 2.35×10^{-13} M, 1000 times higher than that of $\cdot\text{OH}$. These findings are crucial to comprehensively understanding the role of reactive species in the PMC system during the RB21 treatment process.

Acknowledgment. This research was conducted with the financial support of the HNUE science and technology project code SPHN23-17.

REFERENCES

- [1] Yang X, Duan Y, Wang J, Wang H, Liu H & Sedlak DL, (2019). Impact of Peroxymonocarbonate on the Transformation of Organic Contaminants during Hydrogen Peroxide in Situ Chemical Oxidation. *Environmental Science and Technology Letters*, 6(12), 781-786. DOI: 10.1021/acs.estlett.9b00682.

- [2] Xu A, Li X, Xiong H & Yin G, (2011). Efficient degradation of organic pollutants in aqueous solution with bicarbonate-activated hydrogen peroxide. *Chemosphere*, 82(8), 1190-1195. DOI: 10.1016/j.chemosphere.2010.11.066.
- [3] Li Y, Li L, Chen ZX, Zhang J, Gong L, Wang YX, Zhao HQ & Mu Y, (2018). Carbonate-activated hydrogen peroxide oxidation process for azo dye decolorization: Process, kinetics, and mechanisms. *Chemosphere*, 192, 372-378. DOI: 10.1016/j.chemosphere.2017.10.126.
- [4] Zhao T, Li P, Tai C, She J, Yin YY, Qi Y & Zhang Q, (2018). Efficient decolorization of typical azo dyes using low-frequency ultrasound in the presence of carbonate and hydrogen peroxide. *Journal of Hazardous Materials*, 346, 42-51. DOI: 10.1016/j.jhazmat.2017.12.009.
- [5] Xu A, Li X, Ye S, Yin G & Zeng Q, (2011). Catalyzed oxidative degradation of methylene blue by in situ generated cobalt (II)-bicarbonate complexes with hydrogen peroxide. *Applied Catalyst B: Environmental*, 102(1-2), 37-43. DOI: <https://doi.org/10.1016/j.apcatb.2010.11.022>.
- [6] Nguyen TBV, Ho PH, Vu ND, Nguyen BN & Nguyen TH, (2021). Study on the decolorization of Reactive Blue 21 by the peroxymonocarbonate-based oxidation system. *Journal of Analytical Sciences*, 26(6), 175-180 (in Vietnamese).
- [7] Nguyen TBV, Nguyen-Bich N, Vu ND, Ho PH & Nguyen TH, (2021). Degradation of Reactive Blue 19 (RB19) by a green process based on a peroxymonocarbonate oxidation system. *Journal of Analytical Methods in Chemistry*, 2021, ID 6696600, 1-8. DOI: 10.1155/2021/6696600.
- [8] Wang, J & Wang S, (2020). Reactive species in advanced oxidation process: Formation, identification, and reaction mechanism. *Chemical Engineering Journal*, 401, 126158. DOI: 10.1016/j.cej.2020.126158.
- [9] Piechowski MV, Thelen MA, Hoigné J & Bühler RE, (1992). *tert*-Butanol as an OH-Scavenger in the Pulse Radiolysis of Oxygenated Aqueous Systems. *Berichte Der Bunsengesellschaft Für Physikalische Chemie*, 96(10), 1448-1454. DOI: 10.1002/bbpc.19920961019.
- [10] Page SE, Arnold WA & McNeill K, (2010). Terephthalate as a probe for photochemically generated hydroxyl radical. *Journal of Environmental Monitoring*, 12(9):1658-65. DOI: 10.1039/C0EM00160K.
- [11] Huang J & Mabyry SA, (2000). Steady-state concentrations of carbonate radicals in field waters. *Environmental Toxicology and Chemistry*, 19(9), 2181-2188. DOI: 10.1002/etc.5620190906.
- [12] Njus D, Kelley PM, Tu YJ & Schlegel HB, (2020). Ascorbic acid: The chemistry underlying its antioxidant properties. *Free Radical Biology and Medicine*, 159, 37-43. DOI: 10.1016/j.freeradbiomed.2020.07.013.
- [13] Wojnárovits L, Tóth T & Takács E, (2020). Rate constants of carbonate radical anion reactions with molecules of environmental interest in aqueous solution: a review. *Science of the Total Environment*, 717, 137219. DOI: 10.1016/j.scitotenv.2020.137219.